



Exploring the water and carbon monoxide shell around Betelgeuse with VLTI/AMBER

Miguel Montargès, Pierre Kervella, Guy Perrin, Keiichi Ohnaka

► To cite this version:

Miguel Montargès, Pierre Kervella, Guy Perrin, Keiichi Ohnaka. Exploring the water and carbon monoxide shell around Betelgeuse with VLTI/AMBER. Betelgeuse Workshop 2012 The Physics of Red Supergiants: Recent Advances and Open Questions, Nov 2012, Paris, France. pp.167, 10.1051/eas/1360019 . hal-00826849

HAL Id: hal-00826849

<https://hal.science/hal-00826849>

Submitted on 28 May 2013

HAL is a multi-disciplinary open access archive for the deposit and dissemination of scientific research documents, whether they are published or not. The documents may come from teaching and research institutions in France or abroad, or from public or private research centers.

L'archive ouverte pluridisciplinaire **HAL**, est destinée au dépôt et à la diffusion de documents scientifiques de niveau recherche, publiés ou non, émanant des établissements d'enseignement et de recherche français ou étrangers, des laboratoires publics ou privés.

EXPLORING THE WATER AND CARBON MONOXIDE SHELL AROUND BETELGEUSE WITH VLTI/AMBER

M. Montargès¹, P. Kervella¹, G. Perrin¹ and K. Ohnaka²

Abstract. We present the results of the analysis of our recent interferometric observations of Betelgeuse, using the AMBER instrument of the VLTI. Using the medium spectral resolution mode ($R \sim 1500$) we detected the presence of the water vapour and carbon monoxide (CO) molecules in the H and K bands. We also derived the photospheric angular diameter in the continuum. By analysing the depth of the molecular lines and the interferometric visibilities, we derived the column densities of the molecules, as well as the temperature and the size of the corresponding regions in the atmosphere of Betelgeuse (the MOLsphere) using a single shell model around the photosphere. Our results confirm the findings by Perrin *et al.* (2004) and Ohnaka *et al.* (2011) that the H₂O and CO molecules are distributed around Betelgeuse in a MOLsphere extending to approximately 1.3 times the star's photospheric radius.

1 Introduction

Betelgeuse was observed in January and February 2011 with the ESO Very Large Telescope Interferometer (VLTI) using the Astronomical Multi-BEam combineR, AMBER (the instrument is described in Petrov *et al.* 2007) in the *H*-band from 1.45 to 1.80 μm and in the *K*-band from 2.10 to 2.45 μm with the E0-G0-H0, E0-G0-I1 and G0-H0-I1 triplets. The CO and water vapor absorption lines in the *K* band were investigated using the medium spectral resolution of the instrument ($R \sim 1500$).

Based on AMBER observations made with ESO Telescopes at the Paranal Observatory under programmes ID 086.D-0351 and 286.D-5036

¹ LESIA, Observatoire de Paris, CNRS, UPMC, Université Paris-Diderot, 5 place Jules Janssen, 92195 Meudon, France

² Max-Planck-Institut für Radioastronomie, Auf dem Hügel 69, 53121 Bonn, Germany

2 Data reduction

The AMBER data reduction package version 3.0.3 also known as *amdlib* was used to obtain the calibrated interferometric observables (Tatulli *et al.* 2007) : the three visibilities associated to the three baselines are directly the amplitude of the object’s Fourier Transform. It is not possible to measure directly the phase but the calibrated data contain three differential phases (DP) which are sensitive to the photocenter shift in a spectral line with respect to the continuum. The closure phase (CP) is the sum of three phases along the three baselines that form a triangle : $\phi_{CP} = \phi_{12} + \phi_{23} + \phi_{31}$. This quantity is independent from the atmospheric perturbations.

The wavelength calibration was performed using telluric lines in the spectrum of the interferometric calibrator HR-1543 (spectral type F6V). The error bars in the visibilities and closure phases of Betelgeuse were underestimated, probably due to the low visibility of the fringes. We had to split each data file into five subsets to get a new estimation of these errors. We also noticed that some datasets were showing unusually low visibilities : we conclude it was caused by lock loss of the fringe tracker FINITO. These corrupted data sets were discarded.

3 Results

3.1 Continuum analysis

We used two different models to fit the continuum visibilities between 2.1 and 2.245 μm : a uniform disk (UD) and a limb-darkened disk (LDD) using a power law ($I = I_0\mu^\alpha$) according to Hestroffer (1997). We only fitted the data from the first and second lobes in order to avoid contributions from small scale structures at higher spatial frequencies. We used 8752 visibility points over 31 577, from which we derived an angular diameter of $41.01 \pm 0.08 \text{ mas}$ for the uniform disk model giving a reduced χ^2 of 5.27. For the limb-darkened model we obtained an angular diameter of $42.28 \pm 0.09 \text{ mas}$ and a power law coefficient of 0.155 ± 0.005 with a reduced χ^2 of 4.91. The result of these fits is presented in Fig. 1 together with the (u, v) coverage in the first and second lobes. Our value of the angular diameter may not be representative of the average angular diameter of the star as we are only probing one direction of the (u, v) plane.

Our UD value is significantly lower than the previous ones found by Perrin *et al.* (2004) of $43.26 \pm 0.04 \text{ mas}$ and Ohnaka *et al.* (2009 and 2011) of $42.05 \pm 0.05 \text{ mas}$ which was obtained for this later with VLTI/AMBER observations in the same (u, v) direction. This could be caused by the relative decrease of the diameter shown in Ohnaka *et al.* (2011) or by a change in the flux distribution on the photosphere of the star. On the other hand, our LDD value agrees well with the $42.49 \pm 0.06 \text{ mas}$ of Ohnaka *et al.* (2011).

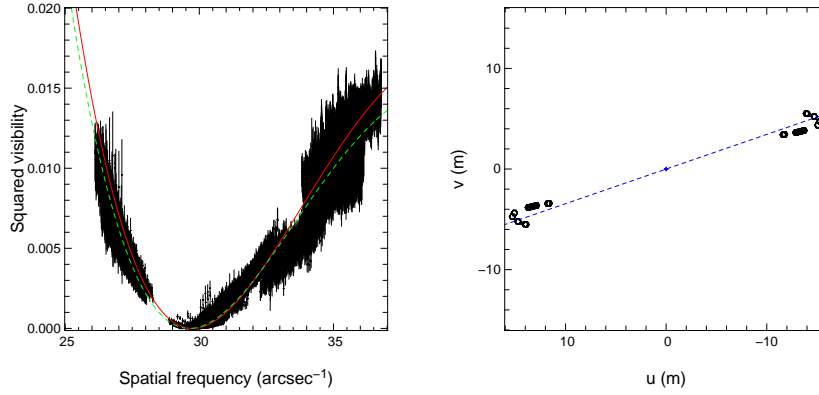


Fig. 1. *Left:* Fit of the continuum squared visibilities. The black points represent the data. The red continuous line is the best fit uniform disk model and the green dashed line is the best fit limb-darkened disk model. *Right:* (u, v) coverage of our AMBER data for the first and second lobes. The blue dashed line represents the average position angle of 73° .

3.2 H_2O and CO absorption lines : model fitting

The wavelengths longer than $2.245 \mu\text{m}$ contain absorption lines from carbon monoxide (CO) and water vapor (H_2O) which are elements present in the MOLsphere described by Tsuji (2000) and Perrin *et al.* (2004). In this paper we restrain ourselves to the first two CO overtone band heads ($2.245 < \lambda < 2.348 \mu\text{m}$). It is clear from Fig. 2 (right panel) that the other bands are not well fitted when these first two are.

We modeled them using a Kurucz atmosphere model¹ (Castelli & Kurucz 2003 and Kurucz 2005) and a single layer containing both CO and H_2O at the same temperature and distance from the photosphere and the corresponding absorptions were computed from the line list of Goorvitch (1994) for CO and from Partridge & Schwenke (1997) for H_2O . This model contains five parameters : the photospheric diameter θ_* , the MOLsphere diameter θ_{MOL} , the MOLsphere temperature T_{MOL} , the CO and H_2O column densities N_{CO} and $N_{\text{H}_2\text{O}}$. Its analytical expression is given by :

$$I_{N_{\text{CO}}, N_{\text{H}_2\text{O}}}(\lambda, \beta) = I_{\text{Kurucz}} e^{\frac{-\tau(N_{\text{CO}}, N_{\text{H}_2\text{O}}; \lambda)}{\cos(\beta)}} + B(\lambda, T_{\text{MOL}}) \left[1 - e^{\frac{-\tau(N_{\text{CO}}, N_{\text{H}_2\text{O}}; \lambda)}{\cos(\beta)}} \right] \quad (3.1)$$

¹<http://kurucz.harvard.edu/>

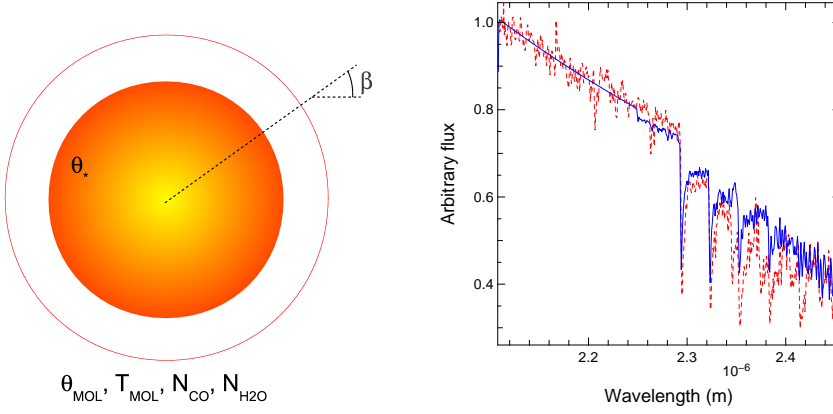


Fig. 2. *Left:* Illustration of the single layer model used to model the MOLsphere. *Right:* The red dashed line is the spectrum obtained from the Betelgeuse AMBER data and the blue continuous line is the spectrum obtained from the single layer model. We used the best fit values from the equation 3.5.

if $\sin(\beta) \leq \frac{\theta_*}{\theta_{\text{MOL}}}$ and otherwise :

$$I_{N_{\text{CO}}, N_{\text{H}_2\text{O}}}(\lambda, \beta) = B(\lambda, T_{\text{MOL}}) \left[1 - e^{\frac{-2\tau(N_{\text{CO}}, N_{\text{H}_2\text{O}}; \lambda)}{\cos(\beta)}} \right] \quad (3.2)$$

$B(\lambda, T)$ is the Planck function, β is the angle between the line of sight and the center of the star and $\tau(N_{\text{CO}}, N_{\text{H}_2\text{O}}; \lambda)$ is the MOLsphere opacity computed from the line lists of Goorvitch (1994) and Partridge & Schwenke (1997). The squared visibility is then derived by computing the Hankel transform of this analytical expression :

$$V_\lambda(x) = \frac{\int_0^1 I(\lambda, r) J_0(rx) r dr}{\int_0^1 I(\lambda, r) r dr} \quad (3.3)$$

With $x = \frac{\pi b \theta_*}{\lambda}$, $r = \sin(\beta)$ and J_0 the zeroth order Bessel function of the first kind.

An illustration of this model and an example of the corresponding spectrum of Betelgeuse model are given in Fig. 2, together with our AMBER observation.

The model contains five *a priori* independent parameters but there are some correlations between T_{MOL} and θ_{MOL} and between the two column densities. Because of this degeneracy, we had to develop a strategy to perform our fit. We fixed θ_* to the value obtained by the uniform disk fit of the continuum data. Then we computed χ^2 maps of our data by fitting N_{CO} and then $N_{\text{H}_2\text{O}}$ at given T_{MOL} and

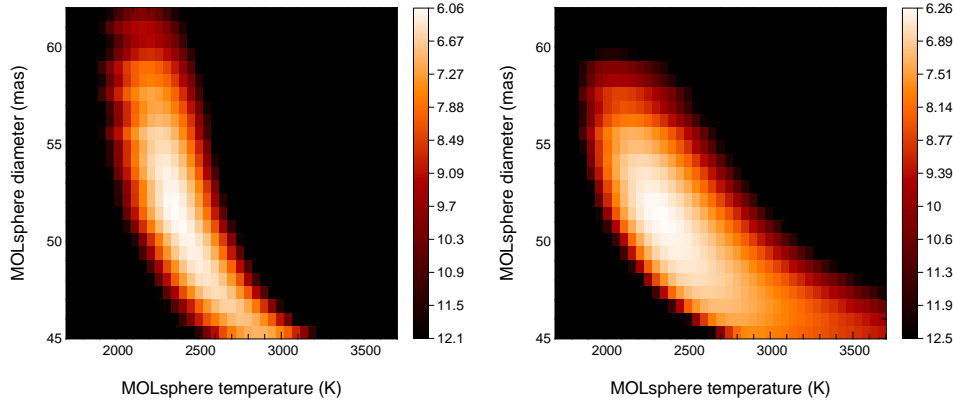


Fig. 3. χ^2 map of the single layer model. *Left:* the CO column density is fitted on each cell of the grid for a constant $N_{H_2O} = 3.28 \times 10^{20} \text{ cm}^{-2}$. *Right:* the H_2O column density is fitted on each cell of the grid for a constant $N_{CO} = 1.53 \times 10^{21} \text{ cm}^{-2}$.

θ_{MOL} :

$$\chi^2(T_{\text{MOL}}, \theta_{\text{MOL}}) = \sum_{i=1}^N \left(\frac{V_i^2 - V_{\text{model}}^2(T_{\text{MOL}}, \theta_{\text{MOL}}, N_{\text{CO}}, N_{\text{H}_2\text{O}}; S_i)}{\sigma_i} \right)^2 \quad (3.4)$$

where S_i is the spatial frequency. N_{CO} and $N_{\text{H}_2\text{O}}$ are fitted on each cell of the grid $(T_{\text{MOL}}, \theta_{\text{MOL}})$. However, there was also a correlation between T_{MOL} and the two column densities. We had to eliminate it by including the spectrum into our fit : this compensates for the lack of interferometric data in the band core caused by the band fringe fitting described in Sect. 2.

The χ^2 maps are presented on Fig. 3 and we derived the following values for the parameters of the MOLsphere :

$$\begin{aligned} T_{\text{MOL}} &= 2300 \pm 50 \text{ K} \\ \theta_{\text{MOL}} &= 51.38 \pm 0.70 \text{ mas} \\ N_{\text{CO}} &= (1.53 \pm 0.6) \times 10^{21} \text{ cm}^{-2} \\ N_{\text{H}_2\text{O}} &= (3.28 \pm 0.7) \times 10^{20} \text{ cm}^{-2} \end{aligned} \quad (3.5)$$

Our two χ^2 maps for carbon monoxide and water vapor present a minimum for the same couple of $(T_{\text{MOL}}, \theta_{\text{MOL}})$. Therefore our hypothesis of a single layer containing both elements is validated. Our best fit values for the angular diameter and the temperature of the MOLsphere are close to those derived by Perrin *et al.* (2004) which were $T_{\text{MOL}} = 2055 \pm 55 \text{ K}$ and $\theta_{\text{MOL}} = 55.78 \pm 0.04 \text{ mas}$.

4 Conclusion

Our analysis of the AMBER visibilities in the continuum allowed us to compute new uniform disk and limb-darkened disk angular diameters. Our absorption line

analysis led us to new values for the MOLsphere parameters, consistent with the results from Perrin *et al.* (2004) and Ohnaka *et al.* (2011).

However, our analysis here only includes data from the first two CO overtone band heads : it must be extended to the other bands, that may probe a deeper molecular layer, closer to the star's photosphere. Finally we will conclude this analysis by exploiting the closure phase signal. This work is currently undergoing and will allow us to search for asymmetries in the light distribution at the surface of the star.

This research has made use of the **AMBER data reduction package** of the Jean-Marie Mariotti Center²

References

- Castelli, F. & Kurucz, R. L. 2003, in IAU Symposium, Uppsala University, Sweden, Vol. 210, Modelling of Stellar Atmospheres, ed. N. Piskunov, W. W. Weiss, & D. F. Gray (ASP), 20
- Goorvitch, D. 1994, ApJS, 95, 535
- Hestroffer, D. 1997, A&A, 327, 199
- Kurucz, R. L. 2005, MmSAI Suppl., 8, 14
- Ohnaka, K., Hofmann, K.-H., Benisty, M. *et al.* 2009, A&A, 503, 183
- Ohnaka, K., Weigelt, G., Millour, F. *et al.* 2011, A&A, 529, A163
- Partridge, H. & Schwenke, D. W. 1997, J. Chem. Phys., 106, 4618
- Perrin, G., Ridgway, S. T., Coudé du Foresto, V. *et al.* 2004, A&A, 418, 675
- Petrov, R. G., Malbet, F., Weigelt, G. *et al.* 2007, A&A, 464, 1
- Tatulli, E., Millour, F., Chelli, A. *et al.* 2007, A&A, 464, 29
- Tsuji, T. 2000, ApJ, 538, 801

²Available at <http://www.jmmc.fr/amberdrs>